

CFD simulation and optimization of ICEs exhaust heat recovery using different coolants and fin dimensions in heat exchanger

M. Hatami · D. D. Ganji · M. Gorji-Bandpy

Received: 23 May 2014 / Accepted: 4 August 2014 / Published online: 17 August 2014
© The Natural Computing Applications Forum 2014

Abstract In this paper, finned type heat exchangers with different fin dimensions in the exhaust of a gasoline engine are modeled numerically for improving the exhaust energy recovery. RNG k - ϵ viscous model is used and the results are compared with available experimental data presented by Lee and Bae (Int J Therm Sci 47:468–478, 2008) where a good agreement is observed. Also, the effect of fin numbers, fin length and three water-based nanofluid coolants (TiO_2 , Fe_2O_3 and CuO) on the heat recovery efficiency are investigated in different engine loads. As a main outcome, results show that increasing the fin numbers and using TiO_2 -water as cold fluid are the most effective methods for heat recover. Furthermore, an optimization analysis is performed to find the best fins dimensions using response surface methodology.

Keywords Response surface method · Waste heat recovery · Heat exchanger · Internal combustion engine · Exhaust

1 Introduction

It is confirmed that in internal combustion engines (ICEs), more than 30–40 % of fuel energy wastes through the exhaust and just 12–25 % of the fuel energy converts to useful work [1, 2]. On the other hand, statistics show that producing amounts of the internal combustion engines

growth very fast and the concern of increasing the harmful greenhouse gases (GHG) will be appeared. So, researchers are motivated to recover the heat from the waste sources in engines using the ways which not only reduce the demand of fossil fuels, but also reduce the GHG and help to energy saving [3, 4]. On the other hand, because exhaust heat exchanger may make a pressure drop and can effect on the engine performance, its design is very important. To select an appropriate heat exchanger design limitations for each heat exchanger type firstly should be considered. Though production cost is often the primary limitation, several other selection aspects such as temperature ranges, pressure limits, thermal performance, pressure drop, fluid flow capacity, cleanability, maintenance, materials, etc. are important. One of the most effective method to increase heat transfer is using the fins which widely used by the researchers [5–9]. Some of the special HEXs designs to recover the exhaust heat are introduced in the following.

Recently, Ghazikhani et al. [10] estimated in an experimental work that brake specific fuel consumption (BSFC) of the diesel engine could be improved approximately 10 % in different load and speeds of an OM314 diesel engine using the recovered exergy from a simple double pipe heat exchanger in exhaust. Pandiyarajan et al. [11] designed a finned-tube heat exchanger and they used a thermal energy storage using cylindrical phase change material (PCM) capsules and found that nearly 10–15 % of fuel power is stored as heat in the combined storage system in different loads. In another experimental work, Lee and Bae [12] designed a little heat exchanger with fins in the exhaust by design of experiment (DOE) technique. They reported that fins should be in the exhaust gases passage for more heat transfer and designed 18 cases in different fins numbers and thicknesses and found the most effective cases. Zhang et al. [13] modeled a finned-tube evaporator

M. Hatami (✉) · D. D. Ganji · M. Gorji-Bandpy
Department of Mechanical Engineering,
Babol University of Technology, Babol, Iran
e-mail: m.hatami2010@gmail.com

D. D. Ganji
e-mail: ddg_davood@yahoo.com

heat exchanger for an Organic Rankine Cycle (ORC). They concluded that waste heat recovery efficiency is between 60 and 70 % for most of the engine's operating region also they mentioned that heat transfer area for a finned-tube evaporator should be selected carefully based on the engine's most typical operating region. Recently, Hossain and Bari [14, 15] applied a new HEX for a diesel engine experimentally and numerically. They applied SST $k-\omega$ for their modeling and they optimized the working fluid pressure and the orientation of heat exchangers and found the additional power increased from 16 to 23.7 %.

A cold fluid or coolant is a fluid which flows through or around a device to prevent its overheating, transferring the heat produced by the device to other devices that use or dissipate it. An ideal coolant has high thermal capacity, low viscosity, is low cost, non-toxic, and chemically inert, neither causing nor promoting corrosion of the cooling system. The most common cold fluid is water. Its high heat capacity and low cost makes it a suitable coolant. It is usually used with additives, like corrosion inhibitors, antifreezes such as ethylene glycol and nanoparticles which make a new class of coolants named nanofluids. Common nanoparticles are CuO, alumina, titanium dioxide, carbon nano-tubes, silica, or metals (e.g. copper or silver) dispersed into the carrier liquid that enhance the heat transfer capabilities compared to the carrier liquid alone [16]. Many studies are performed about using nanofluids as coolant in radiator of engines such as Refs. [17, 18], other applications of nanofluids in heat transfer increasing are presented by authors [19–24].

This paper aims to model the heat transfer through exhaust gases to a cold fluid in a finned heat exchanger numerically to calculate the heat recovery amount and compare with available experimental data. Also, the effects

of water-based nanofluids coolants, fin numbers and fin lengths on energy recovery are investigated in different engine loads.

2 Problem description

As describe before, Lee and Bae [12] optimized a little finned heat exchanger as shown in Fig. 1a for waste heat recovery from exhaust of a gasoline engine. They used a mixture of 50–50 percent of water and ethylene glycol as cold fluid. In the current study, first HEX is modeled numerically, which a schematic of geometry of which is shown in Fig. 1b to validate the results. Then, the effect of fin length, fin number and nanofluids coolants is investigated on the heat recovery amount. Complete information about numerical modeling, boundary layers and assumptions are described in the following section.

3 HEX modeling and analysis

3.1 Numerical modeling

The commercial code FLUENT is adopted to simulate the flow and heat transfer in the computational model. The numerical simulation was performed with a three-dimensional steady-state turbulent flow system. To solve the problem, governing equations for the flow and conjugate heat transfer were modified according to the conditions of the simulation setup. As the problem was assumed to be steady, the time dependent parameters were dropped from the equations. The resulting equations were [25, 26]: Continuity equation:

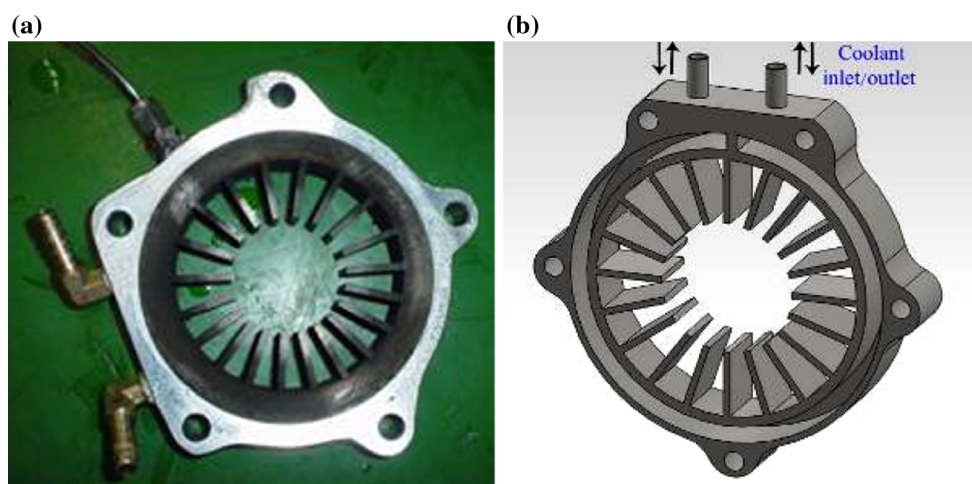


Fig. 1 a Finned heat exchanger designed for exhaust waste heat recovery [12], b Numerical model of (a), investigated in present study

$$\frac{\partial}{\partial x_i}(\rho u_i) = 0 \tag{1}$$

Momentum equations:

$$\frac{\partial}{\partial x_i}(\rho u_i u_k) = \frac{\partial}{\partial x_i} \left(\mu \frac{\partial u_k}{\partial x_i} \right) - \frac{\partial p}{\partial x_k} \tag{2}$$

Energy equation:

$$\frac{\partial}{\partial x_i}(\rho u_i t) = \frac{\partial}{\partial x_i} \left(\frac{k}{C_p} \frac{\partial t}{\partial x_i} \right) \tag{3}$$

In this paper, renormalization-group (RNG) k-ε model is adopted because it can provide improved predictions of near-wall flows and flows with high streamline curvature; also, thermal effect option is selected in the enhanced wall treatment panel. Transport equations for RNG k-ε model in general form are [26]:

Turbulent kinetic energy:

$$\frac{\partial}{\partial t}(\rho k) + \frac{\partial}{\partial x_i}(\rho k u_i) = \frac{\partial}{\partial x_j} \left(\alpha_k \mu_{\text{eff}} \frac{\partial k}{\partial x_j} \right) + G_k + \rho \varepsilon \tag{4}$$

and turbulent energy dissipation:

$$\begin{aligned} \frac{\partial}{\partial t}(\rho \varepsilon) + \frac{\partial}{\partial x_i}(\rho \varepsilon u_i) &= \frac{\partial}{\partial x_j} \left(\alpha_\varepsilon \mu_{\text{eff}} \frac{\partial \varepsilon}{\partial x_j} \right) + C_{1\varepsilon}^* \frac{\varepsilon}{k} G_k \\ &\quad - C_{2\varepsilon} \rho \frac{\varepsilon^2}{k} \end{aligned} \tag{5}$$

where G_k represents the generation of turbulence kinetic energy due to the mean velocity gradients and,

$$\begin{aligned} \mu_{\text{eff}} &= \mu + \mu_t, \mu_t = \rho C_\mu \frac{k^2}{\varepsilon}, C_{1\varepsilon}^* = C_{1\varepsilon}^* - \frac{\eta(1 - \eta/\eta_0)}{1 + \beta\eta^3} \\ \eta &= (2E_{ij} \times E_{ij})^{1/2} \frac{k}{\varepsilon}, E_{ij} = \frac{1}{2} \left[\frac{\partial u_i}{\partial x_j} + \frac{\partial u_j}{\partial x_i} \right]. \end{aligned} \tag{6}$$

The empirical constants for the RNG k-ε model are assigned as following [25, 26]:

$$\begin{aligned} C_\mu &= 0.0845, C_{1\varepsilon} = 1.42, C_{2\varepsilon} = 1.68, \\ \beta &= 0.012, \eta_0 = 4.38, \alpha_k = \alpha_\varepsilon = 1.39. \end{aligned} \tag{7}$$

Transferred heat amount or heat flux is an important parameter in HEX analysis. The average heat flux is [27]

$$\dot{Q}_{\text{ave}} = \frac{(\dot{Q}_g + \dot{Q}_c)}{2} \tag{8}$$

Q_c is the heat transferred to the cold fluid which is calculated as,

$$\dot{Q}_c = \dot{m}_c C_{p,c} (T_{c,\text{out}} - T_{c,\text{in}}) \tag{9}$$

where \dot{m}_c is the mass flow rate of cold fluid and $C_{p,c}$ is the specific heat of cold fluid. Q_g is the heat transferred to exhaust gases which for temperature-dependent specific heat can be calculated as,

$$\dot{Q}_g = \dot{m}_g \int_{T_{g,\text{in}}}^{T_{g,\text{out}}} C_{p,g} dT \tag{10}$$

where \dot{m}_g is the exhaust gases mass flow rate which is the sum of the intake air and fuel consumption mass flow rates [12]. By calculating the Q_{ave} , the overall heat transfer coefficient, U (W/m K) for the HEX can be obtained by [13]

$$U = \frac{\dot{Q}_{\text{ave}}}{L \Delta T_{\text{LMTD}}} \tag{11}$$

where L is the axial length of HEX and ΔT_{LMTD} is the log mean temperature difference, given by

$$\Delta T_{\text{LMTD}} = \frac{\Delta T_{\text{hotend}} - \Delta T_{\text{coldend}}}{\ln \left(\frac{\Delta T_{\text{hotend}}}{\Delta T_{\text{coldend}}} \right)} \tag{12}$$

and ΔT_s are

$$\Delta T_{\text{hotend}} = T_{g,\text{in}} - T_{c,\text{out}} \tag{13}$$

$$\Delta T_{\text{coldend}} = T_{g,\text{out}} - T_{c,\text{in}}. \tag{14}$$

An important parameter which is calculated in the previous works for HEX analysis is HEX effectiveness. Effectiveness can be defined as the ratio of the actual heat transfer in a given HEX to the maximum possible rate of heat transfer, i.e. [14]

$$\varepsilon = \frac{(\dot{m}c_p)_g (T_{c,\text{out}} - T_{c,\text{in}})}{(\dot{m}c_p)_{\text{min}} (T_{g,\text{in}} - T_{c,\text{in}})}. \tag{15}$$

In modeling the nanofluids as coolant, the effective density (ρ_{nf}) is defined as [23]:

$$\rho_{\text{nf}} = \rho_f (1 - \phi) + \rho_s \phi \tag{16}$$

Where ϕ is the solid volume fraction of nanoparticles. Also, the dynamic viscosity of the nanofluids given by Brinkman is [23],

$$\mu_{\text{nf}} = \frac{\mu_f}{(1 - \phi)^{2.5}} \tag{17}$$

the effective thermal conductivity of the nanofluid can be approximated by the Maxwell–Garnetts (MG) model as [23]:

$$\frac{k_{\text{nf}}}{k_f} = \frac{k_s + 2k_f - 2\phi(k_f - k_s)}{k_s + 2k_f + \phi(k_f - k_s)}. \tag{18}$$

3.2 Geometry, mesh generation and boundary conditions

In the numerical modeling, four samples from 18 experiment samples designed in [12] are modeled. Samples 1, 8, 10 and 18 from Ref. [12] are selected due to their maximum and minimum efficiencies. Table 1 presents the complete geometries of these four samples. A mixture of

Table 1 Geometries' characteristics of four samples designed in [12]

Sample number	Coolant flow direction	Fin length (mm)	Fin thickness (mm)	Number of fin	Inner wall thickness (mm)	Length of heat exchanger (mm)	Upper/lower wall thickness (mm)
Sample 1 (1 in [12])	Clockwise	10	1.5	10	2	18	3
Sample 2 (8 in [12])	Clockwise	20	2	20	3	18	5
Sample 3 (10 in [12])	Counter Clockwise	10	1.5	20	4	20	4
Sample 4 (18 in [12])	Counter Clockwise	20	2.5	15	2	20	5

Table 2 Mesh numbers and construction for four samples in Table 1

Samples	Volume 1/cooper	Volume 2/tetrahedral	Volume 3/tetrahedral	Sum of meshes
Sample 1	84,042	98,639	95,576	278,257
Sample 2	76,824	194,326	169,232	440,382
Sample 3	112,740	219,038	154,329	486,107
Sample 4	82,840	158,682	180,849	422,371

50 % water and 50 % ethylene glycol is considered for cold fluid which in samples 1 and 2 circulates clockwise while in samples 3 and 4 circulates counter clockwise. Type and number of generated meshes for these samples are presented through Table 2. Volumes 1, 2 and 3 in Table 2 represent the gases, fins and water mediums, respectively. It's tried to mesh the volume 1 and 2 by structural grids and unstructured mesh is used for volume 3 as shown in Fig. 2. The 3D grid system was established using the GAMBIT commercial code. Also, grid independence tests are carried out to ensure that a nearly grid-independent solution can be obtained. In the test, three different grid systems with approximately 200,000, 400,000 and 600,000 cells are adopted for calculation of the whole heat exchanger, and the difference in the results of two last cases was negligible. As described before, the commercial code FLUENT is adopted to simulate the flow and heat transfer in the computational domain. As reported by Patankar [29], the governing equations are discretized by the finite volume method [25, 26]. The QUICK scheme is used to discretize the convective terms and the SIMPLE algorithm is used to deal with the coupling between velocity and pressure. In the modeling, HEXs are considered well insulated hence the heat losses to the environment are totally neglected. As an approximation, the properties of air can be used for diesel exhaust gas calculations which the error associated with neglecting the combustion products is usually no more than about 2 % [28]. Due to high temperature in exhaust, temperature-dependent properties are considered for exhaust gases and for each property, a fourth-order polynomial is considered whose related equation and coefficients are shown in Table 3. Also, all the solid phases (fins and walls) are made from carbon steel and water-ethylene glycol and nanofluids

are coolants which their properties are presented in Table 4.

3.3 Optimization analysis

3.3.1 Response surface methodology (RSM)

Response surface methodology (RSM) is a collection of mathematical and statistical. Originally, RSM was developed to model experimental responses and then migrated into the modeling of numerical experiments. The difference is in the type of error generated by the response. In physical experiments, inaccuracy can be due, for example, to measurement errors while, in computer experiments, numerical noise is a result of incomplete convergence of iterative processes, round-off errors or the discrete representation of continuous physical phenomena. The application of RSM to design optimization is aimed at reducing the cost of expensive analysis methods (e.g. finite element method or CFD analysis) and their associated numerical noise. Generally, the structure of the relationship between the response and the independent variables is unknown. The first step in RSM is to find a suitable approximation to the true relationship. The most common forms are low-order polynomials (first or second-order). Second-order model can significantly improve the optimization process when a first-order model suffers lack of fit due to interaction between variables and surface curvature. A general second-order model is defined as [30]:

$$y = a_0 + \sum_{i=1}^n a_i x_i + \sum_{i=1}^n a_{ii} x_i^2 + \sum_{i=1}^n \sum_{j=1}^n a_{ij} x_i x_j \Big|_{i < j} \quad (19)$$

where x_i and x_j are the design variables and a are the tuning parameters. CCD or central composite design is one of modules in RSM to obtain the points of each factor according to their levels.

3.3.2 Central composite design (CCD)

A Box-Wilson Central Composite Design, commonly called "central composite design", contains an imbedded factorial or fractional factorial design with center points

Fig. 2 A sample generated mesh for designed heat exchanger

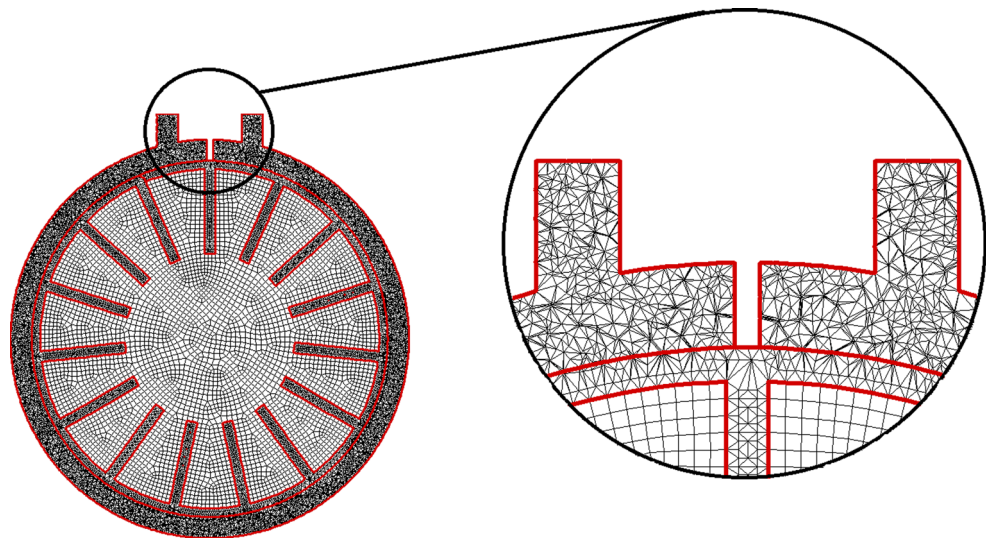


Table 3 Temperature-dependent properties of exhaust gases

Exhaust gas properties	$A + B \times T + C \times T^2 + D \times T^3$			
	A	B	C	D
ρ (kg/m ³)	2.504012288761e + 00	-5.958486188418e-03	5.578942358587e-06	-1.772600918994e-09
C_p (J/kg K)	1.015580935928e + 03	-1.512248401853e-01	4.544870294058e-04	-1.785063817137e-07
μ (kg/m s)	1.325186910351e-06	6.740061370040e-08	-3.749043579926e-11	1.110074961972e-14
k (W/m k)	-3.182421851331e-03	1.185847825677e-04	-7.706004236629e-08	2.939653967062e-11

that are augmented with a group of ‘star points’ that allows estimation of curvature. If the distance from the center of the design space to a factorial point is ± 1 unit for each factor, the distance from the center of the design space to a star point is $\pm \alpha$ with $|\alpha| > 1$. The precise value of α depends on certain properties desired for the design and on the number of factors involved [30, 31].

4 Results and discussions

As mentioned before, four cases of heat exchanger proposed by Lee and Bae [12] are modeled here by RNG k- ϵ viscous model. Although Hatami et al. [32] reviewed all numerical modeling in this area and found that SST k- ω and RNG k- ϵ were more used in the literature, but they [33] showed that RNG k- ϵ is more suitable compared to experimental results. Also, Mokkapati and Lin [34] used this viscous model for modeling the corrugated tube exhaust heat exchanger with twisted tapes inserts. As seen in Fig. 3a, domains which have different densities represent the gas, liquid and solid modeled phases and Fig. 3b confirms that heat conduction through the fins and convection in fluid phases are modeled successfully. To examine the results of numerical modeling, Fig. 4 is

depicted which compares the outlet coolant temperature for all samples with experimental results (left) and for sample 4 (right) in different engine loads. Figure 5 shows the temperature contours for four modeled samples in 20 % load and 4,500 rpm. As revealed by Lee and Bae [12], it seems that samples 1 and 3 (samples 1 and 10 in [12]) have the smallest effectiveness and samples 2 and 4 (8 and 18 in [12]) have the largest cooling effectiveness due to water outlet temperature. By calculating the recovered heat amount, Fig. 6 is depicted for all four samples in different engine loads. As seen, maximum heat recovery is approximately 5,900 W which occurs when engine speed is 4,500 rpm and 100 % load for sample 4 due to higher fin length, thickness and numbers. For this case, by changing just one parameter (fin number or fin length), Fig. 7 is depicted to show the effect of these parameters on heat recovery. It can be seen that effect of increasing the 5 fins is more than increasing the 5 mm to lengths of all fins. Also, as mentioned before nanofluids are suitable coolants, so three nanoparticles are considered to add them to water. TiO₂, Fe₂O₃ and CuO with 0.04 volume fraction are considered and Fig. 8 is depicted after modeling. As shown in this figure, TiO₂ can recover waste heat more than other nanofluid coolants. Finally, for a better conclusion Fig. 9 is presented which show the average of heat recovery

Table 4 Thermal properties of coolants and solid phases [16]

	ρ (kg/m ³)	C_p (J/kg K)	μ (kg/m s)	k (W/m k)
Water	998.2	4,182	0.001003	0.6
Water–Ethylene glycol (50–50)	1,050.44	3,499	0.8 e-03 (in 80 °C)	0.4108
Carbon steel	7,858	486	–	52
TiO ₂	4,250	686.2	–	8.95
Fe ₂ O ₃	5,250	650	–	20
CuO	6,400	531	–	76.5

improvement by different methods in different engine load. As seen, by increasing each 5 fins, 34 % increase in heat recovery will occurred, but it has a limitation due to pressure drop in exhaust. On the other hand, although Water-TiO₂ nanofluid can improve approximately 10 % the heat recovery without pressure drop producing, but it seems that it has more cost than increasing the fin numbers.

As shown in the previous paragraph, fin numbers and height have the most effect on the exhaust heat recover. Because the effect of fin number and height was not very clear, an optimization analysis based on CCD technique is

Fig. 3 3D contour of **a** density and **b** temperatures

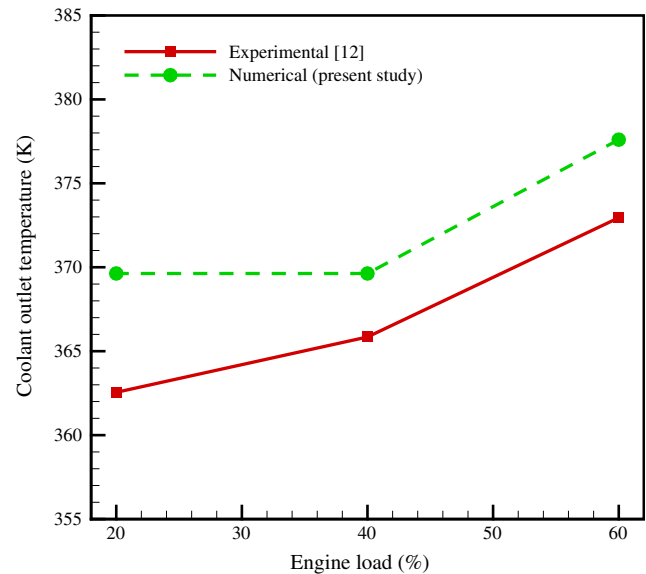
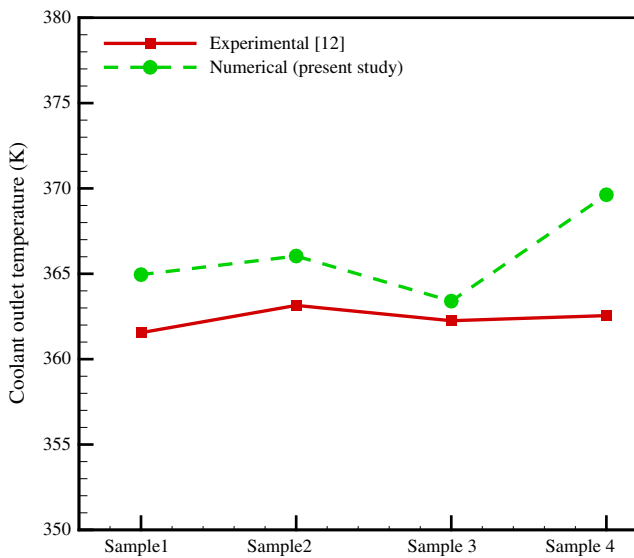
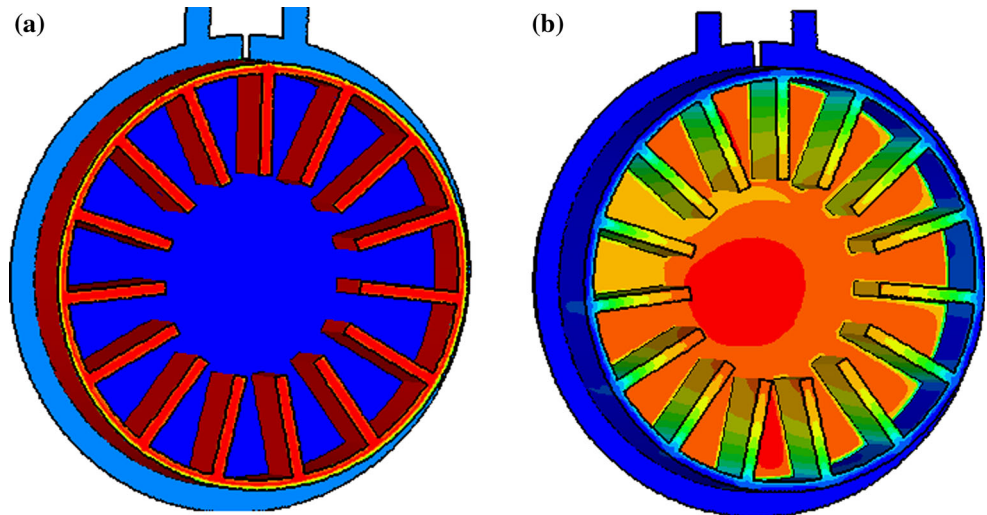


Fig. 4 Comparison of experimental and numerical modeling results

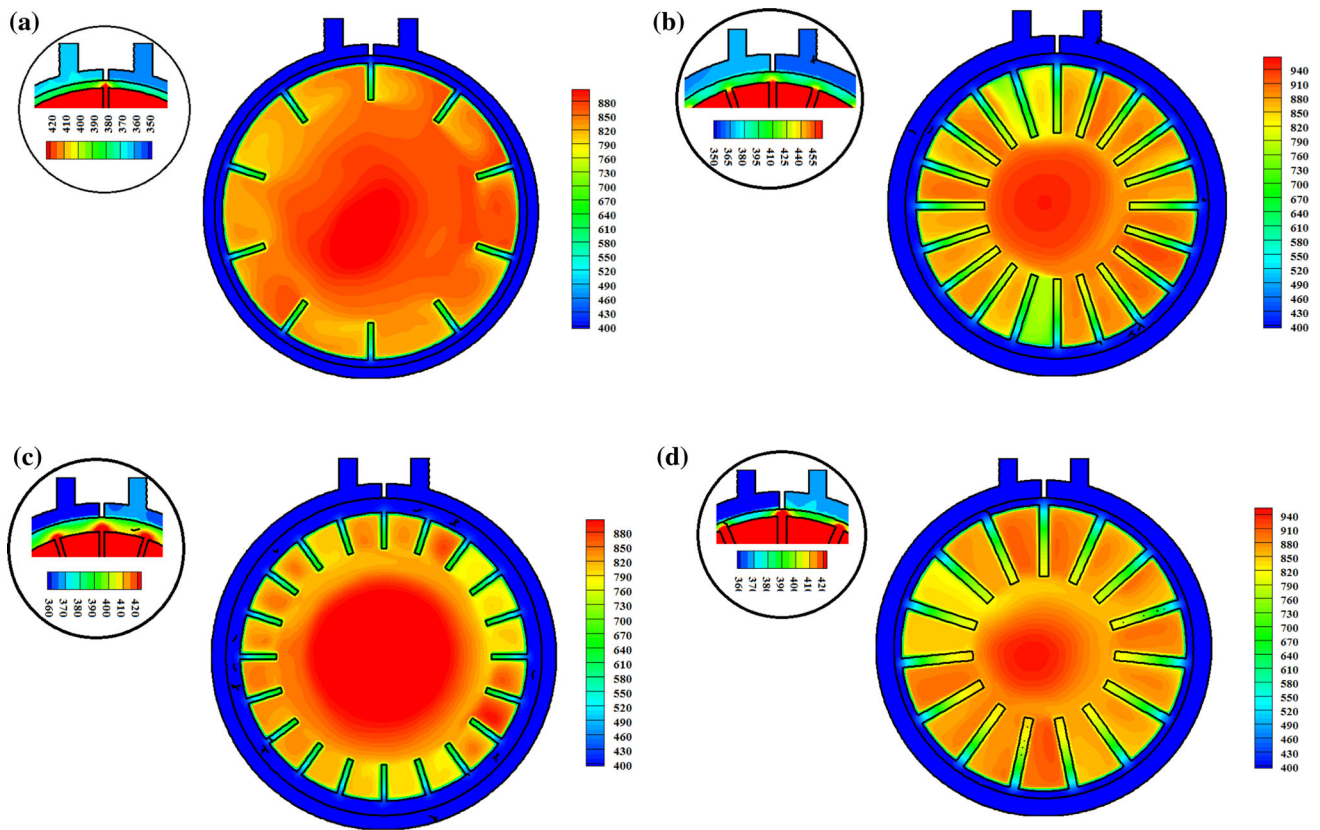


Fig. 5 Temperature contours in 20 % load and 4,500 rpm for **a** sample 1, **b** sample 2, **c** sample 3 and **d** sample 4 (see Table 1)

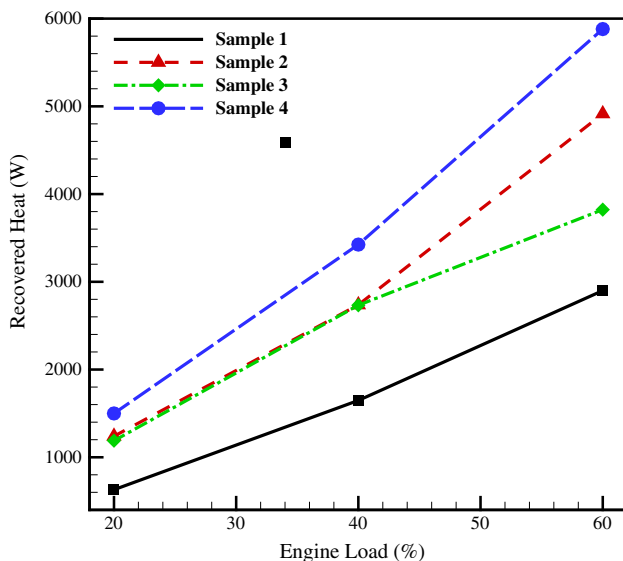


Fig. 6 Recovered heat amount for different samples and engine loads

applied. The +1 and -1 levels for factors are selected as Table 5. By considering five central points, thirteen runs were suggested by the software. Figure 10 which is Box-Cox plot and is obtained from analysis of these points confirms that power transforms is suitable for these data. In

this optimization two responses were considered, weight of the fins and total heat transfer rates. Figure 11 shows the normal plot of the residuals is plotted, obtained from ANOVA (analysis of variance).

Figure 12 is obtained from DOE software based on CCD analysis to show the effects of fin numbers and heights on the responses to find the optimum point of to have maximum heat recovery and minimum weight. In CCD details, α is considered to be unit and five points are considered for central points and two responses are considered for the optimization. Maximum and minimum levels for factors under study are presented in Table 5. In RSM, a polynomial model with cubic order is applied to responses (heat and weight). After considering the power transformation models for analysing the results, R-Squared values are obtained as 0.998 and 1.0 for the transferred heat and weight, respectively. Considering the effects of main factors and also the interactions between two-factor, Eq. (19) takes the form

$$\begin{aligned}
 Q = & 2989.65 + 879.83 \times N + 405.5 \times H \\
 & + 127.72 \times N \times H + 127.06 \times N^2 + 33.61 \times H^2 \\
 & + 17.00 \times N^2 \times H + 19.66 \times N \times H^2
 \end{aligned}
 \tag{20}$$

and for fins weight,

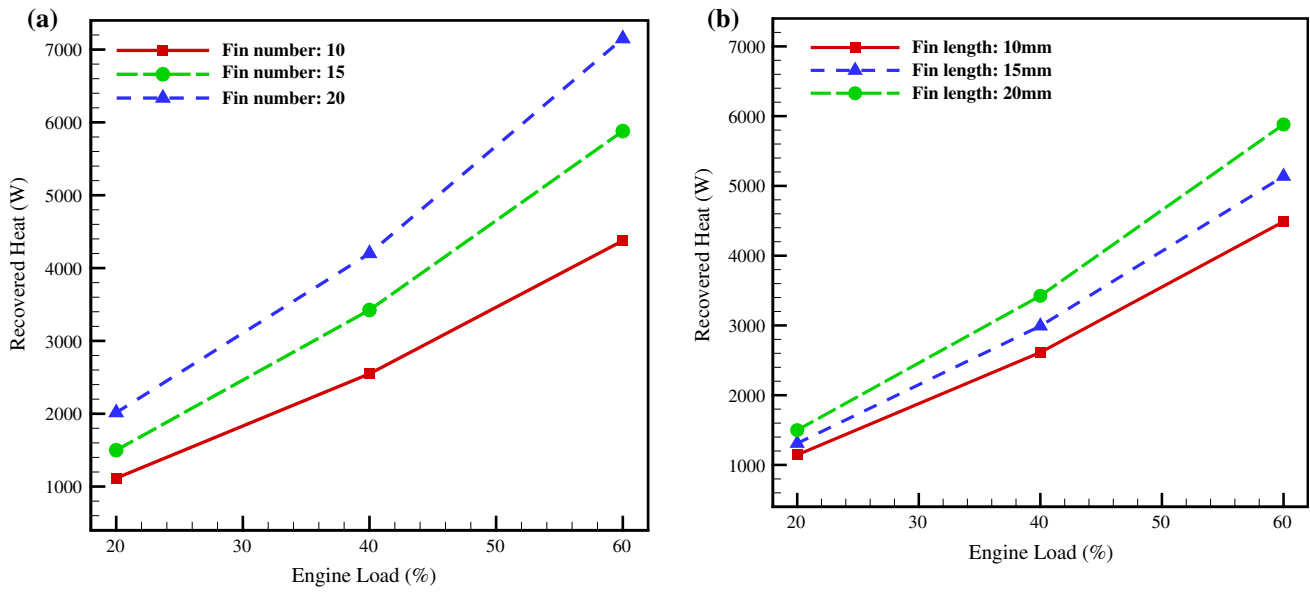


Fig. 7 a Effect of fin numbers and b effect of fins length on recovered heat amount

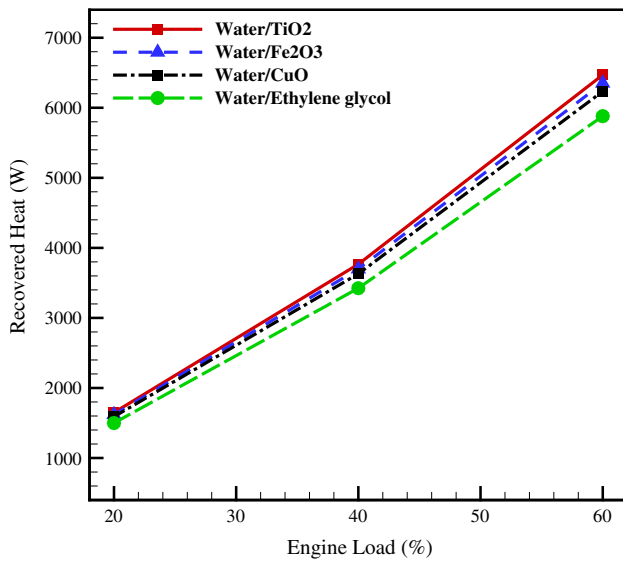


Fig. 8 Effect of different nanofluids coolants on heat recovery

$$W = 0.088 + 0.029 \times N + 0.029 \times H + 0.0098 \times N \times H + 0.00 \times N^2 + 0.00 \times H^2 + 0.00 \times N^2 \times H + 0.00 \times N \times H^2. \quad (21)$$

3D graphs for above formula are shown in Fig. 13 which shows that maximum recovered heat occurs in the maximum levels of factors and minimum weight happens in the minimum levels. Because we want to reach the maximum heat recovery as well as minimum weight, after the CCD analysis, the best heat exchanger designs are presented in Table 6 which desirability contour for the

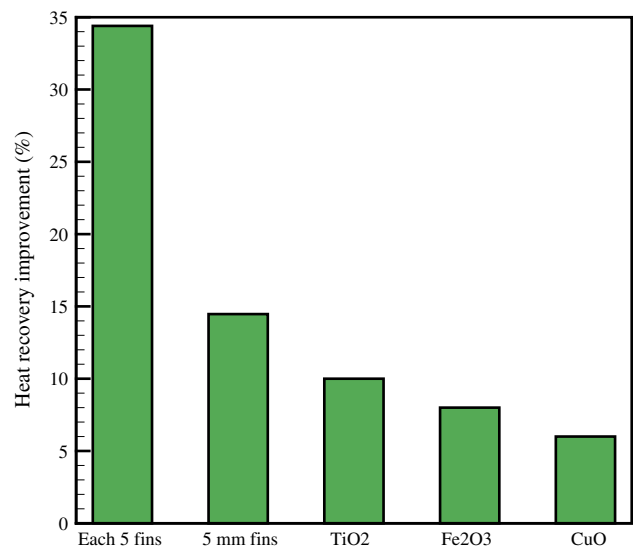


Fig. 9 Average of heat recovery improvement by different methods

Table 5 Level of factors in CCD technique

Factors	Symbol	-1 level	Central point	+1 level
Fin numbers	N	10	15	20
Fin heights (mm)	H	10	15	20

first case is presented in Fig. 14 which predicts the desirability for that optimized point 0.623 as an acceptable optimization.

Fig. 10 Box-Cox plot for power transforms

Design-Expert® Software
(Transferred Heat)^1

Lambda
Current = 1
Best = -1.92
Low C.I. = -2.07
High C.I. = -1.77

Recommend transform:
Power
(Lambda = -1.92)

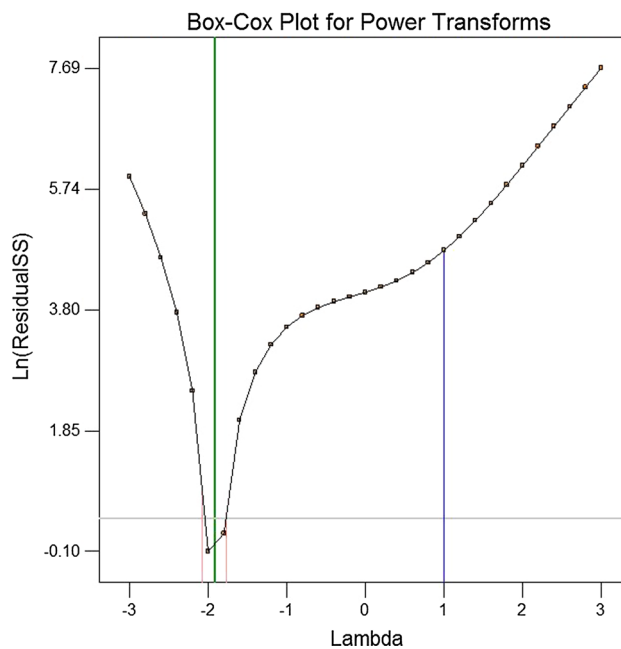
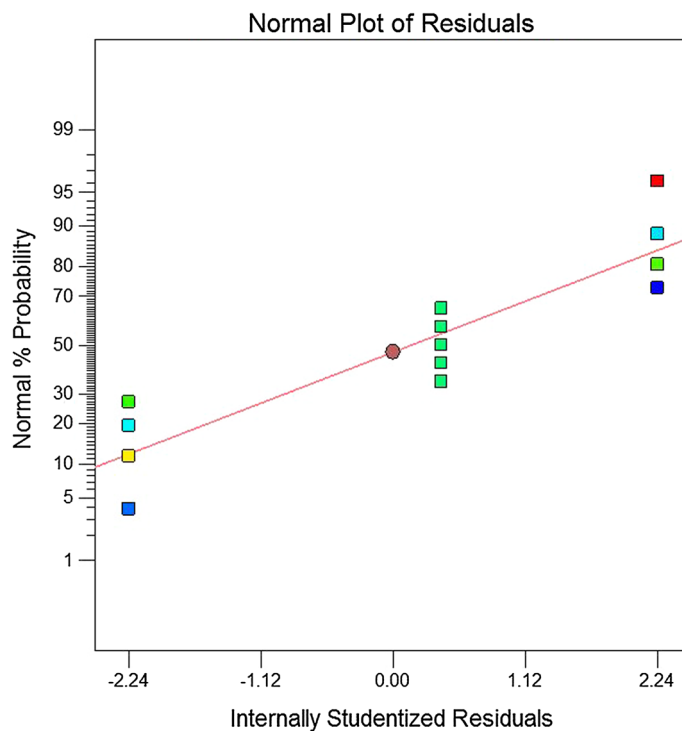


Fig. 11 Normal plot for residuals obtained from ANOVA (analysis of variance)

Design-Expert® Software
(Transferred Heat)^1

Color points by value of
(Transferred Heat)^1:
4602.26
1958.28



5 Conclusion

In this paper, engines exhaust heat is recovered using the finned type heat exchangers numerically. Four types of

experimental HEXs are modeled to examine the numerical results. Results show that RNG k-ε viscous model reaches to an acceptable outcomes compared to experimental data. Also, outcomes reveal that by increasing the each 5 fins,

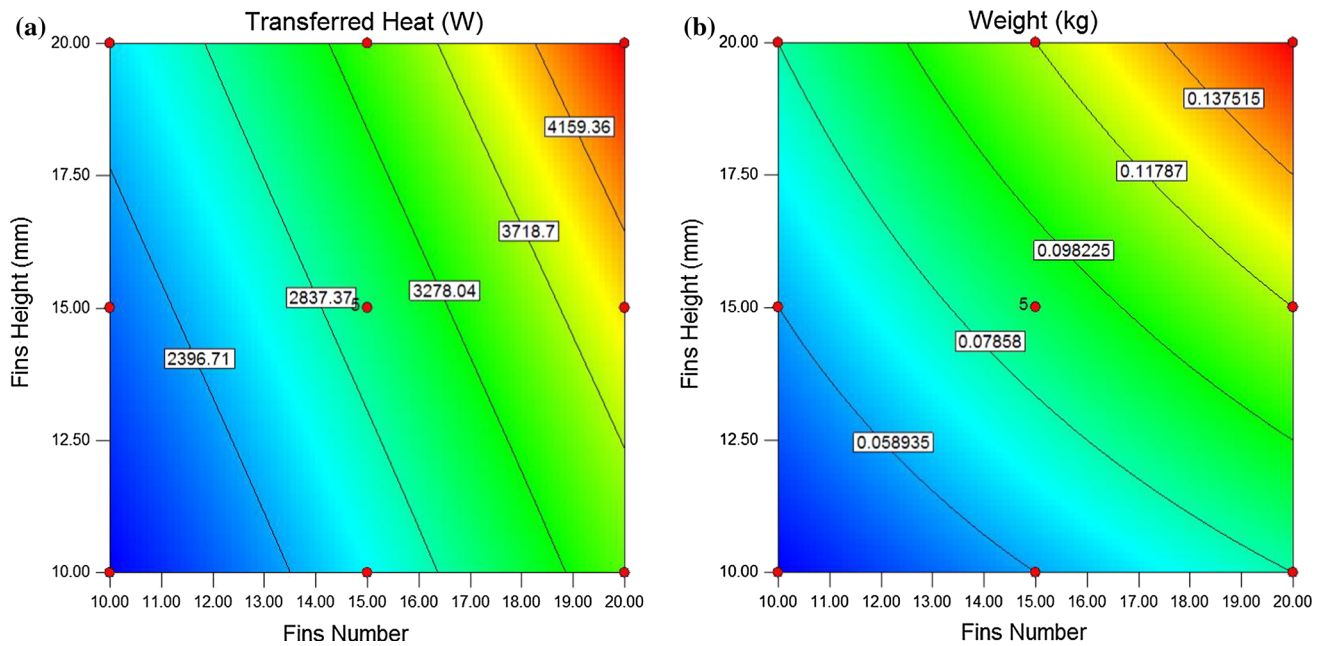


Fig. 12 Contour plots for showing the effect of fin numbers and height on **a** transferred heat and **b** weight

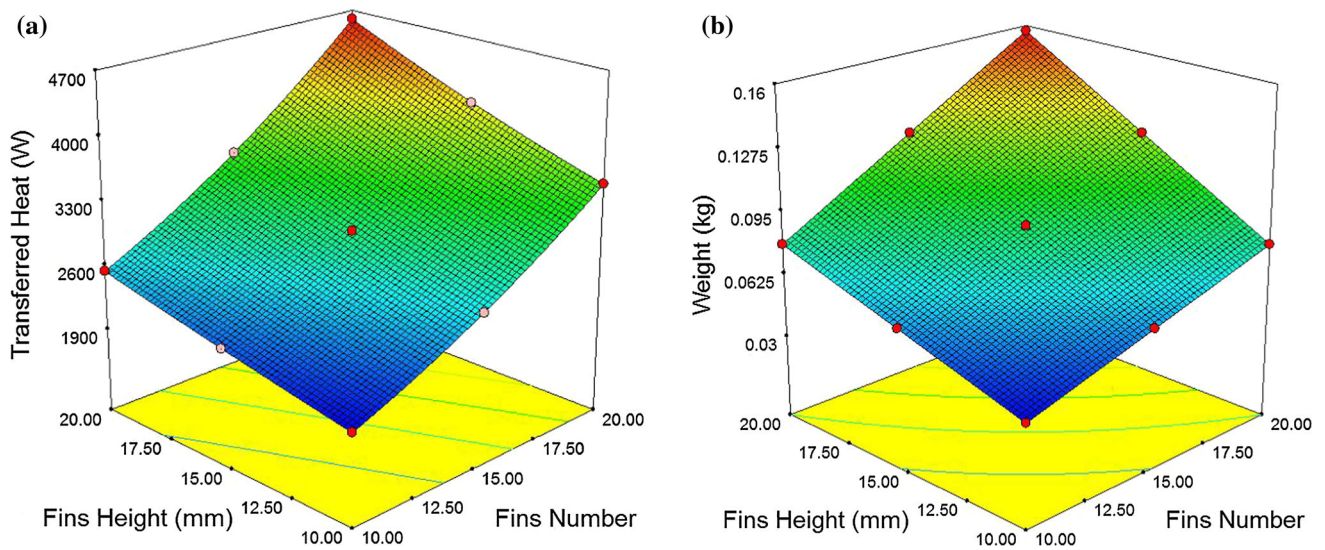


Fig. 13 3D surfaces for **a** recovered heat and **b** weight of fins

Table 6 The best optimized geometries obtained from CCD analysis

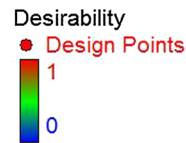
Design number	Fin number	Fin height (mm)	Hear rate (W)	weight (kg)	Desirability	Best design
1	20.00	10.00	3,499.59	0.07858	0.623	✓
2	19.93	10.00	3,486.32	0.0783169	0.622	×

heat recovery improved 34 % averagely but pressure drop also occurs. Furthermore, using the TiO₂-water nanofluid can enhance 10 % in heat recovery although it needs more

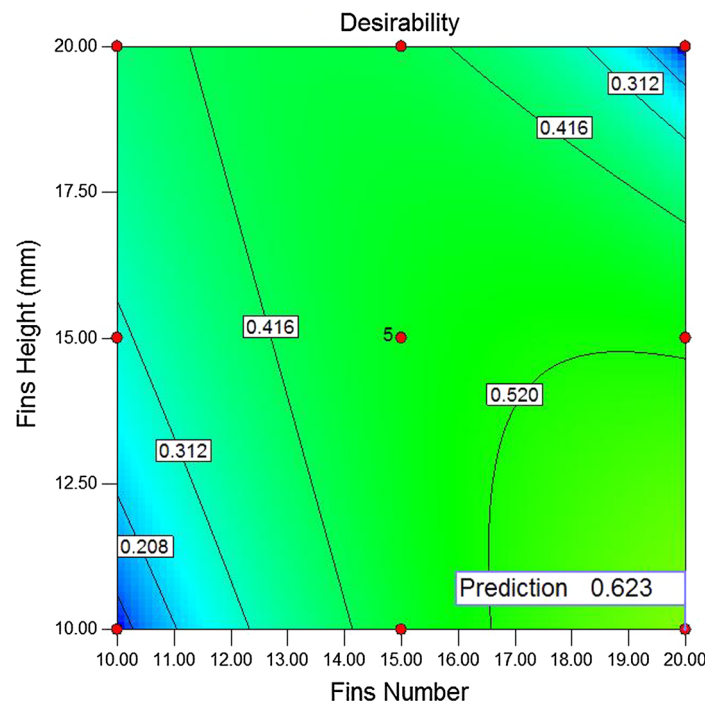
costs. After optimization study using Response Surface Methodology, it is concluded that fin numbers have more effect on heat recovery amount while fin heights have

Fig. 14 Desirability contour for the optimized point

Design-Expert® Software



X1 = A: Fins Number
X2 = B: Fins Height



significant effect on the pressure drop. So, the best design with 20 fin numbers and 10 mm thicknesses was chosen using the CCD technique.

Acknowledgments The authors gratefully acknowledge the respected reviewers for their helpful comments and suggestions. Also, first author (M. Hatami) sincerely appreciates Dr. S. Lee for the experimental data presented in Ref. [12] and his constructive and scientific guidance for validating the results.

References

- Saidur R, Rahim NA, Ping HW, Jahurul MI, Mekhilef S, Masjuki HH (2009) Energy and emission analysis for industrial motors in Malaysia. *Energy Policy* 37(9):3650–3658
- Hasanuzzaman M, Rahim NA, Saidur R, Kazi SN (2011) Energy savings and emissions reductions for rewinding and replacement of industrial motor. *Energy* 36(1):233–240
- Ghazikhani M, Hatami M, Safari B (2014) The effect of alcoholic fuel additives on exergy parameters and emissions in a two stroke gasoline engine. *Arab J Sci Eng*. doi:10.1007/s13369-013-0738-3
- Ghazikhani M, Hatami M, Safari B (2014) Effect of speed and load on exergy recovery in a water-cooled two stroke gasoline-ethanol engine for the bsfc reduction purposes, *Scientia Iranica*, in press, 2014
- Kiwan S, Al-Nimr M (2001) Using porous fins for heat transfer enhancement. *ASME J Heat Transf* 123:2001
- Kiwan S (2007) Effect of radiative losses on the heat transfer from porous fins. *Int J Therm Sci* 46:1046–1055
- Hatami M, Ganji DD (2013) Thermal performance of circular convective-radiative porous fins with different section shapes and materials. *Energy Convers Manag* 76:185–193
- Hatami M, Hasanpour A, Ganji DD (2013) Heat transfer study through porous fins (Si_3N_4 and AL) with temperature-dependent heat generation. *Energy Convers Manag* 74:9–16
- Hatami M, Ganji DD (2014) Thermal and flow analysis of microchannel heat sink (MCHS) cooled by Cu–water nanofluid using porous media approach and least square method. *Energy Convers Manag* 78:347–358
- Ghazikhani M, Hatami M, Ganji DD, Gorji-Bandpy M, Shahi Gh, Behravan A (2014) Exergy recovery from the exhaust cooling in a DI diesel engine for BSFC reduction purposes. *Energy* 65:44–51
- Pandiyarajan V, Chinna Pandian M, Malan E, Velraj R, Seeniraj RV (2011) Experimental investigation on heat recovery from diesel engine exhaust using finned shell and tube heat exchanger and thermal storage system. *Appl Energy* 88:77–87
- Lee S, Bae C (2008) Design of a heat exchanger to reduce the exhaust temperature in a spark-ignition engine. *Int J Therm Sci* 47:468–478
- Zhang HG, Wang EH, Fan BY (2013) Heat transfer analysis of a finned-tube evaporator for engine exhaust heat recovery. *Energy Convers Manag* 65:438–447
- Hossain SN, Bari S (2013) Waste heat recovery from the exhaust of a diesel generator using Rankine cycle. *Energy Convers Manag* 75:141–151
- B S, Hossain SN (2013) Waste heat recovery from a diesel engine using shell and tube heat exchanger. *Appl Therm Eng* 61:355–363
- Reid RC, Prausnitz JM, Poling BE (1987) The properties of gases and liquids, 4th edn. McGraw-Hill, New York
- Peyghambarzadeh SM, Hashemabadi SH, Seifi Jamnani M, Hoseini SM (2011) Improving the cooling performance of automobile radiator with Al_2O_3 /water nanofluid. *Appl Therm Eng* 31:1833–1838
- Leong KY, Saidur R, Kazi SN, Mamun AH (2010) Performance investigation of an automotive car radiator operated with

- nanofluid-based coolants (nanofluid as a coolant in a radiator). *Appl Therm Eng* 30:2685–2692
19. Hatami M, Ganji DD (2014) Thermal and flow analysis of microchannel heat sink (MCHS) cooled by Cu–water nanofluid using porous media approach and least square method. *Energy Convers Manag* 78:347–358
 20. Hatami M, Ganji DD (2013) Heat transfer and flow analysis for SA-TiO₂ non-Newtonian nanofluid passing through the porous media between two coaxial cylinders. *J Mol Liquids* 188:155–161
 21. Hatami M, Nouri R, Ganji DD (2013) Forced convection analysis for MHD Al₂O₃–water nanofluid flow over a horizontal plate. *J Mol Liquids* 187:294–301
 22. Hatami M, Ganji DD (2014) Heat transfer and nanofluid flow in suction and blowing process between parallel disks in presence of variable magnetic field. *J Mol Liquids* 190:159–168
 23. Domairry G, Hatami M (2014) Squeezing Cu–water nanofluid flow analysis between parallel plates by DTM-Padé Method. *J Mol Liquids* 193:37–44
 24. Ahmadi AR, Zahmatkesh A, Hatami M, Ganji DD (2014) A comprehensive analysis of the flow and heat transfer for a nanofluid over an unsteady stretching flat plate. *Powder Technol* 258:125–133
 25. FLUENT 6.3 user's guide (2006) FLUENT Inc., New York
 26. Bilirgen Harun, Dunbar S, Levy EK (2013) Numerical modeling of finned heat exchangers. *Appl Therm Eng* 61:278–288
 27. Rabienataj Darzi AA, Farhadi M, Sedighi K (2013) Heat transfer and flow characteristics of Al₂O₃–water nanofluid in a double tube heat exchanger. *Int Commun Heat Mass Transf* 47:105–112
 28. Perry RH (1984) *Perry's Chemical Engineers' Handbook*, 6th edn. McGraw-Hill, New York
 29. Patankar SV (ed) (1980) *Numerical Heat Transfer and Fluid Flow*. McGrawHill, NewYork
 30. Aslan N (2007) Application of response surface methodology and central composite rotatable design for modeling the influence of some operating variables of a Multi-Gravity Separator for coal cleaning. *Fuel* 86:769–776
 31. Sun Lei, Zhang Chun-Lu (2014) Evaluation of elliptical finned-tube heat exchanger performance using CFD and response surface methodology. *Int J Therm Sci* 75:45–53
 32. Hatami M, Ganji DD, Gorji-Bandpy M (2014) A review of different heat exchangers designs for increasing the diesel exhaust waste heat recovery. *Renew Sustain Energy Rev* 37:168–181
 33. Hatami M, Ganji DD, Gorji-Bandpy M (2014) Numerical study of finned type heat exchangers for ICEs exhaust waste heat recovery. *Case Stud Therm Eng*. doi:[10.1016/j.csite.2014.07.002](https://doi.org/10.1016/j.csite.2014.07.002)
 34. Mokkaapati V, Lin C-S (2014) Numerical study of an exhaust heat recovery system using corrugated tube heat exchanger with twisted tape inserts. *Int Commun Heat Mass Transf*. <http://dx.doi.org/10.1016/j.icheatmasstransfer.2014.07.002>